Influence of the Nano Carbide dispersed Advanced radiation Resistant austenitic stainless Steels (NC-ARES) microstructure on the radiation resistance under ion irradiation

Ji Ho Shin, Byeong Seo Kong, Changheui Jang*, Mike P. Short
Dept. of Nuclear and Quantum Engineering, KAIST, Daejeon, Rep. of Korea
Dept. of Nuclear Science and Engineering, MIT, Cambridge, MA, U.S.A.
*Corresponding Author: chjang@kaist.ac.kr

1. Introduction

The long-term stability of structural materials in highly irradiating environments have been considered a critical issue for future generations of advanced light water reactors [1]. Generally, neutron irradiation of austenitic stainless steels (SSs) used in light water reactors causes radiation damage from displacement cascades [2]. With high-dose (>10dpa) neutron irradiation at relatively high temperature (300–500℃), formations of voids, dislocation loops, and precipitates are the major microstructural changes in austenitic SSs [3]. Especially, voids can cause volumetric swelling (void swelling), which is widely observed in irradiated materials. As a result of that austenitic SSs exhibit radiation-enhanced hardening and embrittlement [2]. Although advanced austenitic SSs, such as Ti modified D9 [4], or NF709 etc.), has been developed, its irradiation resistance remains limited. Fine precipitates have been known to act as efficient traps or sinks for vacancies or interstitial atoms created by neutron irradiation in the various alloys [5]. In addition, dislocations trap vacancies and decrease their super-saturation [6].

Recently, nano carbide dispersed advanced radiation resistant austenitic stainless steel (NC-ARES) was developed to form lots of internal defect trapping sinks to redistribute the concentration of irradiation-induced point defects and their cluster [7]. In this study, irradiation behaviour of the developed alloy, ARES-6, was evaluated for the better understanding of the role of these important metallurgical parameters on the irradiation defects formation mechanisms. To simulate the neutron irradiation, commercial 316 stainless steel (reference) and ARES-6 have been irradiated with heavy ions in the CLASS facility at MIT [8]. Our study shows that the stable defect sinks (large amount of nano-sized NbC precipitates) lead to substantial reduction of dislocation loops and void swelling compared to commercial 316 stainless steels. This study thus provides an important step forward for the further development of advanced radiation tolerant structural steels with the assistance of nano-engineered stable defect sinks.

2. Methods and Results

2.1 Experimental details

The chemical compositions for alloys used in this work are listed in **Table 1**. ARES-6 was developed applying a new approach for forming a high density of uniformly distributed nano-sized carbides in an austenitic SS matrix. Representative TEM image of ARES-6 is presented in **Fig. 1**. The nano-sized NbC precipitates were present, with a mean diameter of approximately 8.4 nm, and number density of approximately $(1.1 \pm 0.3) \times 10^{22}$ /m^3 [7]. Prior to ion irradiation, the surface of the alloys was mechanically polished to a 1 μm followed by electro-polishing at ~20 ℃ at 32 V for 10 s using a 10 % perchloric acid and 90 % acetic acid to remove damaged surface layer. Ni ion irradiations at energy of 5 MeV were performed at 500 ℃ for commercial 316 stainless steel and ARES-6 at (specify ion flux) 2.07×10^{20} ions/m^2 with a defocused beam without raster scanning. The stopping and range of ions in matter (SRIM) method was used to predict the damage profile along the penetration depth by Quick Kinchin Pease Mode method [9], as shown in **Fig. 2**, and the displacement energy 40 eV was used in this calculation [10]. The damage rate values are calculated at 600 nm depth, as represent in **Fig. 2**. The average dose rate and cumulative dose were ~1.8×10^{-3} dpa/s and ~8.5 dpa at this position. This depth was selected to minimize both surface effects and the injected interstitial effect [11].

The irradiated microstructures were examined using transmission electron microscopy (TEM) operated at 200 kV. TEM specimens were prepared using focused ion beam (FIB) performed in a FEI Helios Nanolab 450 using 30 kV. Artifacts induced by FIB were removed by ion polishing with low current (60 pA) and low voltage (5 kV) during the final stage of thinning. Foil thicknesses were determined using the Electron Energy Loss Spectroscopy (EELS) [12].

Table 1 Chemical composition of the 316 SS and ARES-6 (wt.%)

	Fe	Cr	Ni	Mn	Si	Nb	C	Ti	N	Mo
316 SS	Bal.	17.09	10.28	0.58	0.56	-	0.080	-	-	2.14
ARES-6	Bal.	24.13	21.07	1.32	0.23	0.27	0.042	0.023	0.008	-

*ICP-AES, C/S – KS D 1804/1803
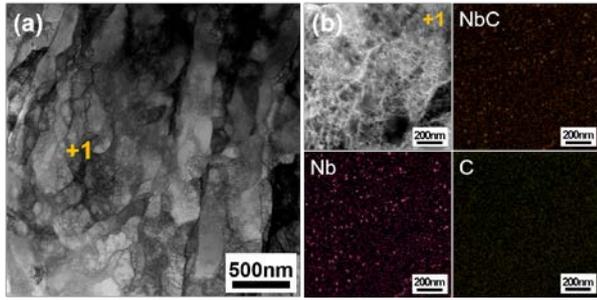
Figure 1 (a) Typical BFTEM image of ARES-6. (b) HAADF and EDS mapping images for point 1 in the BFTEM image (a)
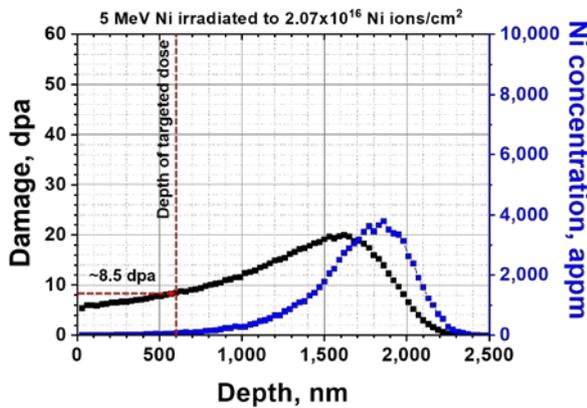
Figure 2 Damage profile (black line) and Ni implantation (blue line) computed with SRIM

2.2 Irradiation resistance

Vacancies and interstitial atoms are primary lattice defects that cause observable microstructural changes, such as the formation of dislocation loops and voids in crystalline solids. **Figure 3** shows cross-sectional bright field TEM images of 316 SS (**Fig. 3**a) and ARES-6 (**Fig. 3**b) microstructure after Ni ion beam irradiation to 8.5 dpa (600 nm from the surface) at 500 ℃. The cross-section micrograph shows ranges from the outer surface (indicated with red dashed lines in each case) to 1 μm. Since the irradiation experiment resulted primarily in the formation of dislocation loops, the rel-rod dark-field (DF) imaging technique was employed to characterize dislocation loops. The [011] zone axis was selected and tiled to a two-beam condition, and specific diffraction pattern image is located in **Fig. 3**a and b respectively.

A quantification of the dislocation (faulted) loop density and the size distribution was performed to compare the microstructural evolution of the alloys after heavy ion irradiation. For loop density calculation, images were contrast adjusted and a binary threshold level was manually set using Image-J [13]. Rel-rod DFTEM micrographs were analyzed from the 500−700 nm depth region for each alloy, then the average loop diameter and the number density were calculated in same region in these micrographs and the results are

presented in **Table 2**. Irradiated 316 SS had large amount of dislocation loops (($(0.45 \pm 0.2) \times 10^{22}$ /m^3), while ARES-6 showed relatively low number density of dislocation loops (($(0.07 \pm 0.03) \times 10^{22}$ /m^3). Since formation of dislocation loops is very biased sinks [14], irradiated 316 SS which has high number density of dislocation loops would increase the vacancy supersaturation region. Meanwhile, ARES-6 can dramatically reduce the magnitude of void swelling compared with irradiated 316 SS. However, fabricated TEM specimen by FIB was too thick to perform quantitative analysis regarding the density of voids. When it comes to voids, further analysis (FIB fabrication and TEM analysis) will be carried out.
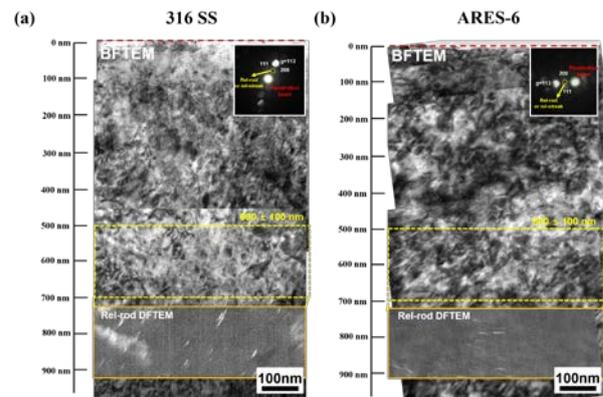
Figure 3 (a) Panoramic cross-section TEM micrograph of Ni ion irradiated commercial 316 SS showing a large number of dislocation loops. (b) Cross-section TEM overview of irradiated ARES-6 showing much less dislocation loops. In both alloys, the 600 ± 100 nm regions are outlined by the yellow dashed lines. In addition, dislocation loops analyzed by rel-rod DFTEM are highlighted by orange lines corresponding to same region with yellow dashed lines.

Table 2 TEM quantification of dislocation loops after irradiation with 5 MeV Ni at 500 ℃ (500−700 nm depth)

Material	Dislocation loop (Frank loop)	
	D_{ave} (nm)	ρ_{loop} ($\times 10^{22}$ m^{-3})^a
Type 316 SS	27.3 ± 8.7	0.45 ± 0.2
ARES-6	56.6 ± 15.4	0.07 ± 0.3

^{a} 1/4 of loops were counted and results were multiplied with four

3. Summary

The irradiation resistance of a newly developed ARES-6 and commercial 316 SS was evaluated by using the Ni heavy ion irradiation. An ARES-6 alloy containing a high density of uniformly distributed nano-sized carbides in austenitic matrix showed significant reduction in the amount of dislocation loops in austenitic matrix. The present study implies that ARES-6 has promising potential for applications in extreme radiation environments. Meanwhile, additional analysis

will be performed to quantitively evaluate the void swelling of each alloy.

REFERENCES

[1] M.K. Miller et al., The effects of irradiation, annealing and reirradiation on RPV steels, J. Nucl. Mater. 351 (2006), pp. 216-222

[2] J. Gan et al., Microstructure evolution in austenitic Fe–Cr–Ni alloys irradiated with rotons: comparison with neutron-irradiated microstructures, J. Nucl. Mater. 297 (2001), pp. 161-175

[3] S.J. Zinkle et al., Dose dependence of the microstructural evolution in neutron-irradiated austenitic stainless steel, J. Nucl. Mater. 206 (1993), pp. 266-286

[4] S.J. Zinkle et al., Materials challenges in nuclear energy, Acta Mater. 61 (2013), pp. 735-758

[5] E. Lee et al., Fe–15Ni–13Cr austenitic stainless steels for fission and fusion reactor applications. III. Phase stability during heavy ion irradiation, J. Nucl. Mater. 278 (2000), pp. 20-29

[6] A. Renault et al., Correlation of radiation-induced changes in microstructure/microchemistry, density and thermo-electric power of type 304L and 316 stainless steels irradiated in the Phénix reactor, J. Nucl. Mater. 460 (2015), pp. 72-81

[7] J.H. Shin et al., Development of thermo-mechanical processing to form high density of uniformly distributed nanosized carbides in austenitic stainless steels, Mater. Sci. Eng. A 775 (2020), pp. 138986

[8] C.A. Dennett et al., Real-time thermomechanical property monitoring during ion beam irradiation using in situ transient grating spectroscopy, Nucl. Instrum. Methods Phys. Res., Sect. B 440 (2019), pp. 126-138

[9] J.F. Ziegler et al., The stopping and range of ions in solids, Pergamon, New York, 1985

[10] ASTM Standard E693-01, Standard practice for characterizing neutron exposure in iron and low alloy steels in terms of displacements per atom, 2001.

[11] E. Getto et al., Effect of pre-implanted helium on void swelling evolution in self-ion irradiated HT9, J. Nucl. Mater. 462 (2015), pp. 458-469

[12] T. Malis et al., EELS log-ratio technique for specimen-thickness measurement in the TEM, J Electron Microsc Tech 8 (1988), pp. 193-200

[13] C.A. Schneider et al., NIH Image to ImageJ: 25 years of image analysis, Nat. Meth. 9 (2012), pp. 671-675

[14] J.J. Hoyt et al., The solute dependence of bias factors in irradiated Fe-Ni alloys, 179-181 (1991), pp. 1096-1099